Study of carrier recombination transient characteristics in MOCVD grown GaN dependent on layer thickness

E. Gaubas, T. Čeponis, A. Jasiunas, E. Jelmakas, S. Juršėnas, A. Kadys, T. Malinauskas, A. Tekorius, and P. Vitta

Citation: AIP Advances **3**, 112128 (2013); doi: 10.1063/1.4835056
View online: http://dx.doi.org/10.1063/1.4835056
View Table of Contents: http://scitation.aip.org/content/aip/journal/adva/3/11?ver=pdfcov
Published by the AIP Publishing

Articles you may be interested in
Optical and structural studies of homoepitaxially grown m-plane GaN
Appl. Phys. Lett. **100**, 172108 (2012); 10.1063/1.4706258

Growth and optical and structural characterizations of GaN on freestanding GaN substrates with an (Al,In)N insertion layer
Appl. Phys. Lett. **89**, 191912 (2006); 10.1063/1.2385113

Stress control in GaN grown on silicon (111) by metalorganic vapor phase epitaxy
Appl. Phys. Lett. **79**, 3230 (2001); 10.1063/1.1415043

Single-phase hexagonal GaN grown on AlAs/GaAs(001)
Appl. Phys. Lett. **77**, 244 (2000); 10.1063/1.126938

Optical spectroscopy of GaN grown by metalorganic vapor phase epitaxy using indium surfactant
Appl. Phys. Lett. **76**, 3388 (2000); 10.1063/1.126655

NEW Special Topic Sections
NOW ONLINE
Lithium Niobate Properties and Applications: Reviews of Emerging Trends
AIP Applied Physics Reviews

Reuse of AIP Publishing content is subject to the terms at: https://publishing.aip.org/authors/rights-and-permissions. Download to IP: 158.129.154.116 On: Wed, 24 Aug 2016 07:35:45

Study of carrier recombination transient characteristics in MOCVD grown GaN dependent on layer thickness

E. Gaubas,[a] T. Čeponis, A. Jasiunas, E. Jelmakas, S. Juršėnas, A. Kadys, T. Malinauskas, A. Tekorius, and P. Vitta
Institute of Applied Research, Vilnius University, Sauletekio Ave. 9-III, LT-10222, Vilnius, Lithuania

(Received 24 July 2013; accepted 12 November 2013; published online 21 November 2013)

The MOCVD grown GaN epi-layers of different thickness have been examined in order to clarify a role of surface recombination, to separate an impact of radiative and non-radiative recombination and disorder factors. The microwave probed –photoconductivity (MW-PC) and spectrally resolved photo-luminescence (PL) transients were simultaneously recorded under ultraviolet (UV) light 354 nm pulsed 500 ps excitation. The MW-PC transients exhibited the carrier decay components associated with carrier decay within micro-crystals and the disordered structure on the periphery areas surrounding crystalline columns. Three PL bands were resolved within PL spectrum, namely, the exciton ascribed UV-PL band edge for $h\nu > 3.3$ eV, blue B-PL band for $2.5 < h\nu < 3.0$ eV and yellow Y-PL band with $h\nu < 2.4$ eV. It has been obtained that intensity of UV-PL band increases with excitation density, while intensity of B-PL band is nearly invariant. However, intensity of the Y-PL increases with reduction of the excitation density. The Y-PL can be associated with trapping centers. A reduction of UV excitation density leads to a decrease of the relative amplitude of the asymptotic component within the MW-PC transients and to an increase of the amplitude as well as duration of the yellow spectral band (Y-PL) asymptotic component. Fractional index α with values $0.5 < \alpha < 0.8$ was evaluated for the stretched-exponent component which fits the experimental transients determined by the disordered structure ascribed to the periphery areas surrounding the crystalline columns. © *2013 Author(s). All article content, except where otherwise noted, is licensed under a Creative Commons Attribution 3.0 Unported License.*
[http://dx.doi.org/10.1063/1.4835056]

I. INTRODUCTION

GaN is intensively developed for optoelectronics and power device applications.[1–4] GaN is also a promising material for radiation hard particle detectors operating in harsh environment of irradiations.[5–8] To support the sufficient charge collection efficiency within a detector volume, the rather thick layers of detector base region should be used in design of the diode type particle detectors. Also, the large resistivity material is desirable to form the active area of the particle detector. Significant problems appear in formation of junctions and electrodes on GaN,[9] caused by contamination with metals during metallization and due to their interplay with the intrinsic grown-in defects of high density. Up-to-now, rather high density of dislocations is inherent for GaN layers grown by MOCVD technology. Thereby, dislocation nets may introduce the disorder inherent carrier transport and recombination effects.[10] The disorder can be a reason for the stretched-exponent relaxation (SER) type transients[3,4,10–13] in photoconductivity (PC) and photo-luminescence (PL) decay. These phenomena are often accompanied by the persistent photoconductivity,[11,12] barrier mediated carrier trapping,[10] photoconductivity quenching[11] effects. These effects[3,4,11–13]

[a]Author to whom correspondence should be addressed. Electronic mail: eugenijus.gaubas@ff.vu.lt

 © Author(s) 2013

Reuse of AIP Publishing content is subject to the terms at: https://publishing.aip.org/authors/rights-and-permissions. Download to IP: 158.129.154.116 On: Wed, 24 Aug 2016 07:35:45

TABLE I. Parameters of samples extracted by Hall effect and HRXRD measurements.

Sample number made/under regime	Layer thickness (μm)	Carrier density (cm^{-3})	Carrier mobility (cm^2/Vs)	Threading dislocation density (cm^{-2})
1047 TU/1047 °C	2.4	n/a	n/a	$>10^{10}$
950 TU/ 950 °C	2.4	n/a	n/a	$>10^{10}$
925 TU/ 925 °C	2.4	n/a	n/a	$>10^{10}$
53 VU/1070 °C	2.5	4.5×10^{17}	199 ± 3	1.3×10^9
38 VU/1070 °C	5.6	4.2×10^{17}	191 ± 3	8.6×10^8
181 VU/1070 °C	13.1	8.7×10^{16}	210 ± 6	6.2×10^8
184 VU/1070 °C	19.5	4.0×10^{16}	214 ± 6	5.1×10^8
185 VU/1070 °C	25.5	2.9×10^{16}	190 ± 6	4.8×10^8

and interpretation of the photoluminescence spectral bands[3,4,11–14] are commonly considered on the basis of the point defect analysis by including the defect transforms in configurational space,[11] temperature dependent changes of trap activation energy[13] and carrier decay lifetime, extracted from the SER fits of the experimental time resolved PL and PC transients.[11–13] However, existence of the disorder inherent PL and PC effects necessitates clarifying of the role of carrier transport and capture dynamics. In MOCVD grown GaN epi-layers, averaged density of dislocations exceeds values of 10^8 cm^{-2}, therefore their role cannot be ignored in analysis of the barrier associated carrier capture, the radiative recombination transitions involving dislocation core ascribed deep levels,[10] the space charge regions surrounding dislocation cores, and the dislocation nets caused carrier random-walk diffusion-limited[15] carrier transport and trapping effects.

In this work, the epi-layers of different thickness of the MOCVD grown GaN on sapphire substrates have been studied in order to clarify the role of surface recombination, to separate the impact of the radiative and non-radiative recombination parameters and the disorder factors. The time and spectrum resolved contactless methods of the photoluminescence (PL) and microwave probed photoconductivity (MW-PC) were combined for the synchronous measurements in order to control a performance of the radiative and non-radiative recombination channels.

II. SAMPLES AND MEASUREMENT TECHNIQUES

A set of wafer pieces of 2.4–25.5 μm thickness n-GaN un-intentionally doped epi-layers grown by the metal-organic chemical vapor deposition (MOCVD) on sapphire substrates was investigated. For comparison, a few samples (2.4 μm thick) grown by Tokushima University (TU) MOCVD reactor and the different thickness GaN epi-layers grown by MOCVD reactor at Vilnius University (VU) were simultaneously investigated. The thick layers (VU) were grown by using longer growth time. The sample parameters evaluated by Hall and high resolution X-ray diffraction (HRXRD) measurements are listed in Table I.

As can be deduced from the Table I, the density of free carriers varies reciprocally relative to an epi-layer thickness. This implies that the effective density of the rather shallow donor-type traps decreases with enhancement of a crystal volume. Such a behavior requires a clarification whether these traps are localized at the layer surfaces, which role is reduced with enhancement of a layer thickness, i.e. the ratio of the surface area to the crystal bulk. The measured values of carrier mobility can be assumed to be invariable in the range of experimental errors of 10%. This hints that the grown-in defects make a rather weak impact on carrier scattering, while being the efficient recombination centers responsible for the luminescence.

The crystallinity of GaN epi-layers has been controlled by X-ray reflections from crystal planes using XRD measurements, e.g. Ref. 15. The XRD rocking curves (w-scans) at (001) and (302) reflections were measured to determine the threading dislocation density (TDD) in GaN films.[16] The TD density has been evaluated assuming a random distribution of dislocations and using a formalism described in Refs. 17 and 18. In order to determine density of screw and edge type dislocations, the XRD rocking curves (w-scans) have been examined at (0002) and (30-32) reflections. The FWHM

Reuse of AIP Publishing content is subject to the terms at: https://publishing.aip.org/authors/rights-and-permissions. Download to IP: 158.129.154.116 On: Wed, 24 Aug 2016 07:35:45

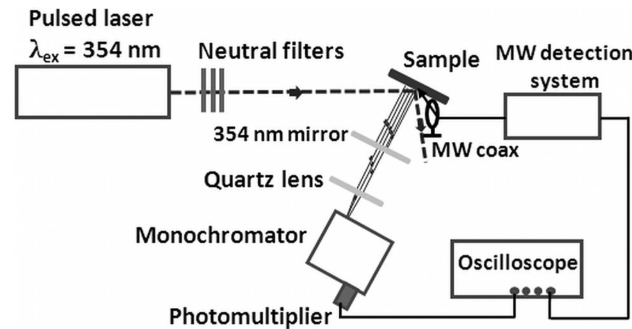

FIG. 1. A setup of the instrumentation for the simultaneous measurements of the MW-PC and PL spectrum resolved transients.

of the (0002) w-scans show density of screw dislocations, while broadening of the (30-32) reflection in GaN is almost solely determined by edge type dislocation.[16] The total threading dislocation density (TDD), estimated by XRD and verified by EBIC[19–21] (electron beam induced current scans performed on a few samples containing Schottky barriers) measurements, is also presented in Table I. It can be noticed that the highest TD density is inherent for the TU made GaN layers, while this TD density decreases reciprocally to the layer thickness in VU grown GaN epi-layers. TDD changes more than two times over the entire range of the examined layer thicknesses in the VU made samples. However, these samples, especially the TU grown epi-layers, should be considered as a rather dislocation-rich material with TDD $> 5 \times 10^8$ cm^{-2}.

A sketch of the experimental arrangement for the simultaneous microwave probed photoconductivity (MW-PC) and photoluminescence (PL) spectrum - time resolved measurements at room temperature is shown in Fig. 1.

The transient signals of the MW-PC and PL have been synchronously measured by collecting a response of the same UV (354 nm) excitation beam spot, generated by a micro-chip laser STA-1-TH ("Standa") employed for the pulsed (500 ps) excitation of the excess carriers. The excitation density is varied by spectrally neutral optical filters in the range of 0.001 – 2 μJ/cm^2. The MW-PC response has been detected by using a coaxial needle-tip probe and a near field probing regime, performed by a VU made instrument VUTEG-3. A microwave reflection mode has been implemented in these measurements. The registered signal is transferred from VUTEG-3 to a digital 1GHz oscilloscope Tektronix TDS-5104, equipped with a computer, where MW-PC transient is displayed and processed. The PL light is collected from the area with normal directed towards a bisector between the incident and the reflected UV light beams. The UV filtered PL light is focused onto a slit of a Jobin Yvon monochromator. The PL light is displayed using a grating within the monochromator, and the PL pulsed signal is detected by a Hamamatsu H10721 photomultiplier. This PL signal is also transferred to another channel of the digital oscilloscope TDS-5104, where the PL transient is displayed and processed together with MW-PC transient.

III. RESULTS AND DISCUSSION

A. The time resolved characteristics of photoluminescence and photoconductivity

The initial photoconductivity decay component appears in the same time domain relative to the radiative recombination kinetics in GaN layers (Fig. 2). Duration of the U_{PL} decay comprises $\tau_{r,i} \approx 2.3$ ns evaluated within a relaxation stage of the PL transient at a level $\exp(-1) \approx 0.368$ of the normalized amplitude of PL signal.

Therefore, to distinguish the carrier decay rates ascribed to the micro-crystals (where UV-PL is the most efficient) and the periphery surrounding the monocrystalline volumes, a subtraction procedure (illustrated in Fig. 2) for the normalized PL and MW-PC signals can be applied for a rough primary estimation of the impact of radiative (*r*) and non-radiative (*nr*) channels. The

Reuse of AIP Publishing content is subject to the terms at: https://publishing.aip.org/authors/rights-and-permissions. Download to IP: 158.129.154.116 On: Wed, 24 Aug 2016 07:35:45

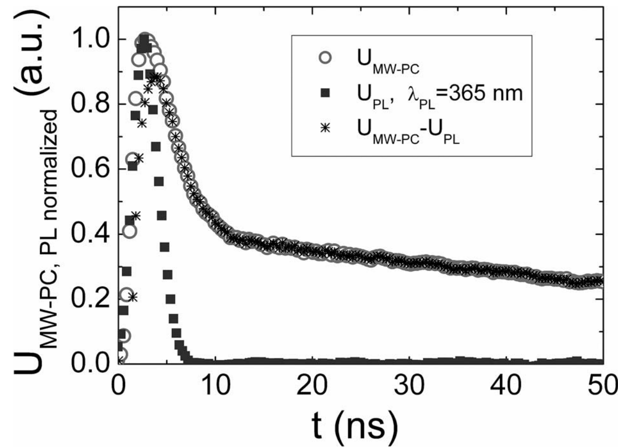

FIG. 2. The MW-PC decay transient displayed within an initial stage of the MW-PC signal relaxation compared with a simultaneously registered PL transient at 365 nm PL wavelength in the 5.6 μm thick epi-layer.

overlapped components of carrier decay through the radiative and non-radiative recombination within a system of distributed parameters are mediated through carrier diffusion. Then, MW-PC signal (which amplitude $U_{MW\text{-}PC}$ is proportional to the excess carrier density n, i.e. $U_{MW\text{-}PC} \sim n$) can be approximated by synchronous linear (non-radiative $\sim n$) and non-linear (radiative $\sim n^2$) processes. In this case, a decay of the excess carrier density in time t is generally described by continuity equation $\partial n/\partial t = D\partial^2 n/\partial y^2 - n/\tau_{nr} - \gamma n^2$ with parameters of the carrier diffusion coefficient D along spatial coordinate y, of the characteristic time of non-radiative decay τ_{nr}, of the coefficient γ of radiative recombination using relevant boundary conditions (e.g. of a type $D\partial n/\partial y|_{y0} = sn$) on surface ($y = y_0$ with surface recombination velocity s). The continuity equation can be solved analytically only at approach of the instantaneous decay time $\tau_{r,i} = 1/\gamma n$ for radiative recombination. Solution of this equation can be approximated by a sum $n(t) = n(t=0)\sum_{m,i} A_m \exp[-(\eta_m{}^2 D + 1/\tau_{nr})t]\exp[-(1/\tau_{r,i})t_i]$ over the spatial frequencies[22–24] η_m and instantaneous lifetimes $\tau_{r,i}$. Replacing the sum by an integral averaged over duration $\tau_{MW\text{-}PC}$ of the MW-PC decay and keeping in mind linearity of the detection regime ($U_{MW\text{-}PC} \sim n(t)$), the MW-PC transient can be described (through normalized,-subscript *norm*, amplitudes of the non-radiative (nr) and radiative (r) recombination components) by expression $U_{MW\text{-}PC}(t) \approx [U_{MW\text{-}PC,0}/\tau_{MW\text{-}PC}]\int U_{nr,norm}(t)U_{r,norm}(t-\Theta)d\Theta$. Assuming $U_{r,norm} \approx U_{PL,norm}$ and $U_{MW\text{-}PC,0} = U_{MW\text{-}PC}(t-\Theta=0)$, the differential MW-PC component ascribed to the non-radiative decay $U^{s}{}_{\text{MW-PC,nr}}(t) = U_{MW\text{-}PC}(t=0) - [U_{MW\text{-}PC,0}/\tau_{MW\text{-}PC}]\int U_{nr,norm}(t)U_{PL,norm}(t - \Theta)d\Theta$ leads to an approach:

$$U^{s}_{MW-PC,nr}(t)\} = \frac{1}{\tau_{MW-PC}}\int_0^t [1 - U_{PL}(\Theta)]U_{MW-PC}(t-\Theta)d\Theta$$

$$\approx \frac{1}{\tau_{PL}}\int_0^{\tau_{PL}} [1 - U_{PL}(\Theta)]U_{MW-PC}(t-\Theta)d\Theta + U_{MW-PC}(t > \tau_{PL}).$$

The obtained differential signal is shown by stars in Fig. 2. This differential signal $U^{s}{}_{MW\text{-}PC,nr}$ (a residual MW-PC signal) can then be attributed to the peripheral areas of a multi-crystalline material. The elimination ($U_{MW\text{-}PC} - U_{PL}$) of this PL decay component from the integral MW-PC signal ($U_{MW\text{-}PC}$) leads to decrease of the initial amplitude of the normalized ($U^{s}{}_{MW\text{-}PC} \sim U_{MW\text{-}PC} - U_{PL}$) component. This $U^{s}{}_{MW\text{-}PC}$ component coincides with MW-PC transient after UV-PL signal disappears (within a linear scale). This result implies that the micro-volumes within a multi-crystalline GaN layer coincide (for which the MW-PC and PL signals are synchronously collected and

Reuse of AIP Publishing content is subject to the terms at: https://publishing.aip.org/authors/rights-and-permissions. Download to IP: 158.129.154.116 On: Wed, 24 Aug 2016 07:35:45

exhibit the fast decay components in MW-PC and PL transients). Thus, it can be assumed that the slower (than $\tau_{r,i}$ in U_{PL}) MW-PC initial component $U^{s}{}_{MW\text{-}PC}$ is ascribed to the stretched-exponent decay, and it appears due to carrier brought to a periphery of the monocrystalline micro-volumes (columns) within a GaN epi-layer. The dislocations are namely located within these periphery areas surrounding the crystalline columns. The excess carriers, brought to the periphery areas with space charge regions within Cottrell spheres/cylinders of dislocations, are separated by the space charge field.

Thus, the excess carrier recombination is only mediated by carrier diffusion, caused by the excess carrier density gradients. Thereby, these different (fast and slow) carrier decay components should be ascribed to the different micro-areas of the epi-GaN material. To collect the MW-PC and PL signal from the same excited volume (where the lateral micro-inhomogeneity of material is inevitable), the synchronous detection of the MW-PC and PL responses is necessary in order to highlight the impact of the radiative and non-radiative carrier decay. The transient MW-PC signals, integrated from the excited area, contain the overlapped components of carrier decay through the radiative and non-radiative recombination.

The initial component of the MW-PC transients is in the same time scale as that of the PL transients measured for the different PL wavelengths (Fig. 3). A reduction of the UV excitation intensity leads to a decrease of the amplitude of the asymptotic component within the MW-PC transients. This can be understood as the potential barrier mediated carrier trapping.[10] The reduction of excitation intensity also leads to a shortening of the initial MW-PC decay component, as illustrated in Fig. 3(a). This hints a decrease of the impact of the radiative recombination (PL) within the MW-PC signal, as a rather small excess carrier part decays through the radiative channels, due to a limited efficiency of the PL. This simultaneously indicates an increase of the role of carrier trapping centers. The carrier trapping processes are however mediated (limited) by diffusion,[10,25] for a small density of the mobile carriers in the disordered peripheral areas of the multicrystalline material. The barrier and diffusion limited trapping[10,25] leads to the long (in a millisecond time scale), non-exponential relaxation of the MW-PC signal (Fig. 3(a)).

The UV-PL (exciton attributed) intensity follows a reduction of the UV excitation density. However, the reduction of the UV excitation intensity causes an enhancement of the Y-PL amplitude and asymptotic component duration, as can be inferred from Fig. 3(b). Nevertheless, the measurable Y-PL signal can only be obtained in the scale of hundred microseconds in the time resolved PL at wavelengths $\lambda_{PL} \geq 525$ nm. Additionally, the long tail PL relaxation component weakens for the shorter wavelength PL, $\lambda_{PL} < 500$ nm (Fig. 3(c)). These observations can be understood at assumption that the non-linear, barrier mediated carrier trapping centers (associated with the non-exponential MW-PC relaxation) could be related to the B-PL radiative recombination. A reduction of excitation density leads to an enhancement of the barrier and to the decrease of the asymptotic component within the MW-PC transients. The B-PL radiative recombination channel governs then the excess carriers involved into the space charge region which surrounds a dislocation core, if B-PL can be attributed to the radiative recombination through the deep levels ascribed to the dislocation core. At this assumption, the intensity of B-PL radiative recombination is weakly dependent on excess carrier density, provided the excitation density is insufficient to considerably modify the potential barrier ascribed to a dislocation. Consequently, a competing channel, as the sub-system levels of the donor-acceptor (D-A) type point defects ascribed to the Y-PL radiative recombination,[14] becomes a prevailing one. These traps seem to be located in the periphery of the micro-crystals, and the carriers, diffusion brought to a micro-crystal boundary, determine the component of the fast Y-PL decay. The impact of carriers photo-generated in the micro-crystals is thereby reduced within the entire Y-PL signal with a decrease of excitation intensity (Fig. 3(b)). The role of the Y-PL centers localized at surface of a micro-crystal is equalized to influence of those existing in the periphery of the micro-crystals, for the small density of the photo-excited carriers. Then, the relative impact of the Y-PL centers located in the periphery of the micro-crystals increases with reduction of excitation density, and this leads to the enhancement of the relative amplitude of the Y-PL and stretched-exponent (SER) type relaxation. The latter SER trapping process is governed and limited by random-walk of small density mobile carriers in the disordered peripheral areas.

Reuse of AIP Publishing content is subject to the terms at: https://publishing.aip.org/authors/rights-and-permissions. Download to IP: 158.129.154.116 On: Wed, 24 Aug 2016 07:35:45

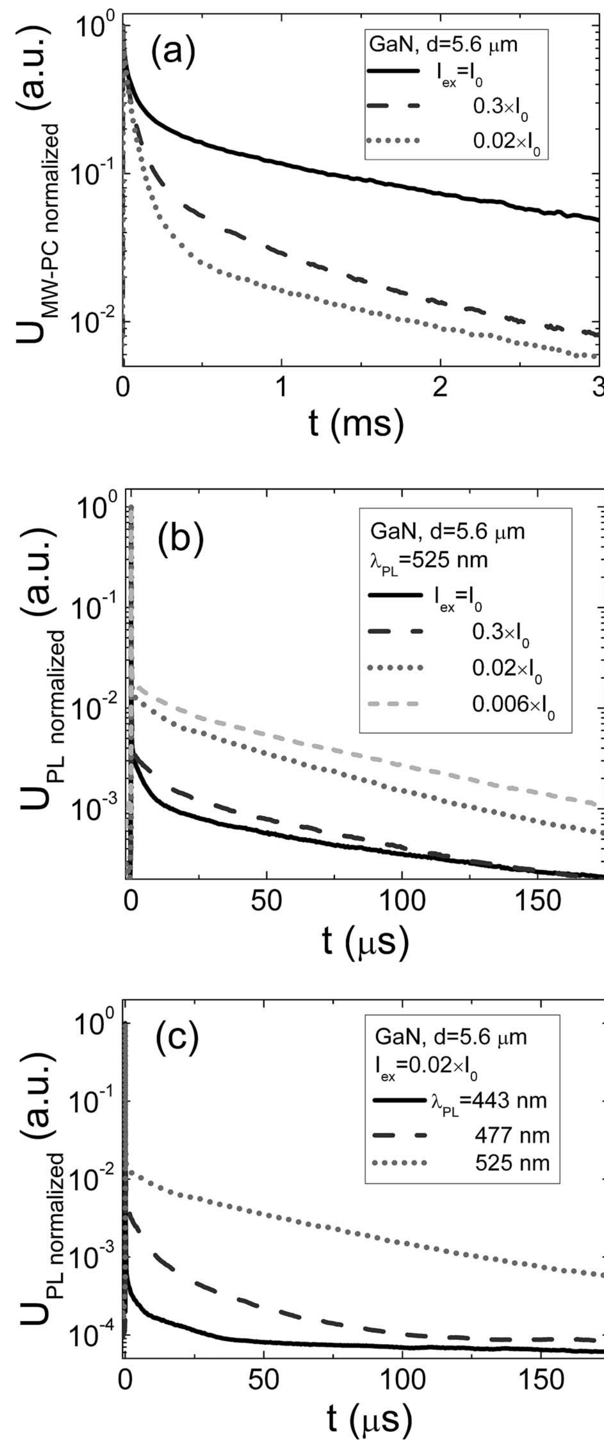

FIG. 3. The MW-PC transients (a) and PL decay transients at 525 nm wavelength (b) measured varying excitation intensity and luminescence wavelength (c) in 5.6 μm thick GaN epi-layer.

B. Spectral characteristics of the photoluminescence dependent on layer thickness

The registered PL amplitudes (extracted from the PL transients dispersed at fixed wavelength) as a function of the PL quantum energy ($h\nu$) are plotted in Fig. 4. Several PL bands can be resolved within a PL spectrum: namely, the exciton ascribed UV-PL band appearing for $h\nu > 3.3$

Reuse of AIP Publishing content is subject to the terms at: https://publishing.aip.org/authors/rights-and-permissions. Download to IP: 158.129.154.116 On: Wed, 24 Aug 2016 07:35:45

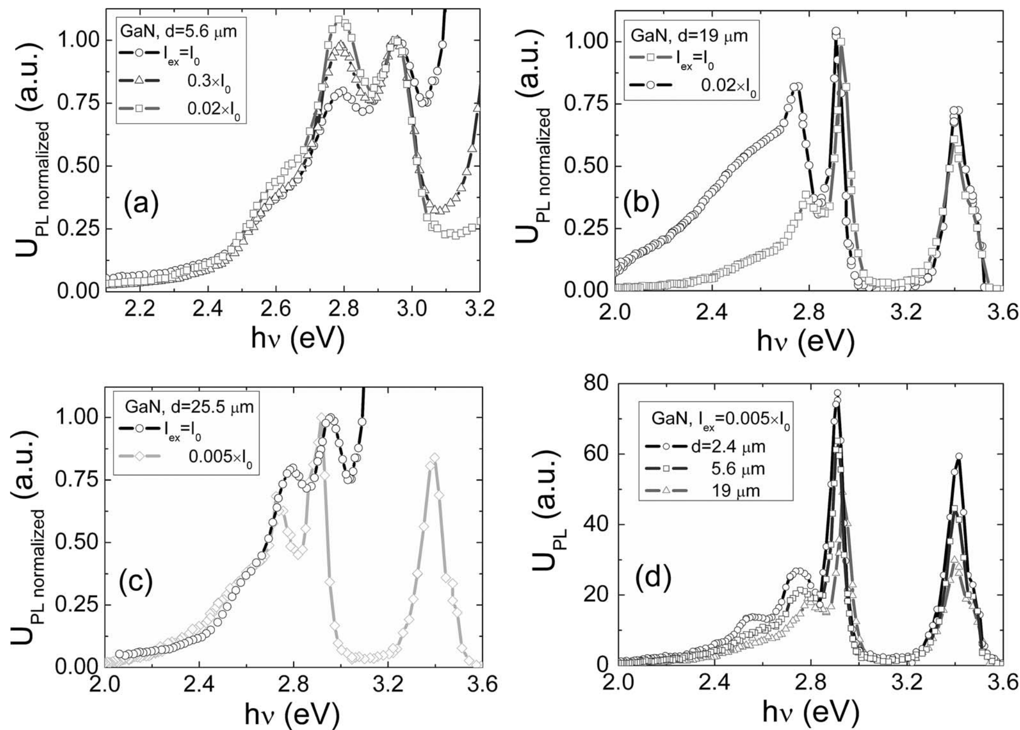

FIG. 4. Spectral variations of the normalized amplitude of the PL transients measured at different excitation densities on different thickness (d) GaN samples: (a) $d = 5.6$ μm; (b) $d = 19$ μm; (c) $d = 25.5$ μm; (d) at fixed I_{ex} for $d = 2.4$, 5.6, and 19 μm.

eV, the defects attributed bands of blue B-PL (for $2.5 < h\nu < 3.0$ eV) and the yellow Y-PL (with $h\nu < 2.4$ eV). These PL bands are well examined,[14,26–33] thereby our spectroscopy results correlate with literature data. It can be deduced from the comparison of these spectra measured at different excitation densities that the intensity of the UV-PL band increases with excitation density, while the intensity of B-PL band is nearly invariant, but the intensity of the Y-PL increases with reduction of excitation density.

This clearly indicates that the role of the Y-PL is enhanced with reduction of the excess carrier density, and it can be associated with the carrier trapping centers, being a sub-system of D-A radiative recombination, interpreted in detail.[14] Carrier trapping centers, as usual, act together with the recombination ones. For the large initial excess carrier density within conduction/valence band, the main carrier capture flow runs through the deep recombination centers, while the shallower trapping centers are filling with excess carriers. During these processes, the density of excess carriers in conduction band can become either an equal or less relative to that on the shallow trapping centers. Then, the recombination process is proceeded on a support of the carriers thermally generated from the trapping centers. A reduction of the initial excess carrier density (being proportional to the excitation intensity) highlights the impact of the trapping centers in PL transients. The trapped carriers can proceed their existence either being thermally released to conduction band or captured to the deeper center. The latter process is then responsible for the D-A radiative recombination. Such the scenarios can be ascribed to the Y-PL behavior in our observations by correlating results on PL and MW-PC transients. These results are in the qualitative agreement with literature data.[26–33]

The B-PL band is also interpreted[14] as the D-A transitions ascribed to the different origin defects (relative to Y-PL). In our experiments, the nearly invariant intensity of the B-PL band transients has been obtained when changing the excitation density. Therefore, the PL spectra (in Fig. 4) were normalized to peak amplitude of the B-PL band. The spectral position of the B-PL peak is also stable and independent of the epi-layer thickness, while an appearance of the UV-PL and Y-PL depends on layer thickness. The changes of the UV-PL intensity relative to that of B-PL in rather thick layers

Reuse of AIP Publishing content is subject to the terms at: https://publishing.aip.org/authors/rights-and-permissions. Download to IP: 158.129.154.116 On: Wed, 24 Aug 2016 07:35:45

can be explained by the re-absorption effect for PL radiation wavelengths close to the threshold of interband transitions. The B-PL intensity slightly increases with excitation density irrespective of the epi-layer thickness (Fig. 4(d)), while the intensity of the UV-PL and Y-PL (Figs. 4(a)–4(c)) changes considerably and non-linearly with excitation intensity in epi-layers of different thickness. The absolute values of the B-PL intensity decrease with an increase of the epi-layer thickness, and this is in agreement with reduction of TDD (Table I), reciprocally dependent on layer thickness. For a fixed excitation intensity (Fig. 4(d)), the density of defects, responsible for both the Y-PL and B-PL, decreases with enhancement of the epi-layer thickness. This implies that quality of the epi-layer improves with increase of layer thickness.

The time and spectrum resolved changes of the B-PL, being different from that of Y-PL, hint on different origin of these B-PL defects. The main candidate, as a B-PL center, would be dislocations, which are inevitable even in the rather thick MOCVD-grown GaN layers.[10] The interpretation[14] of the B-PL through the D-A type recombination is not contradicted in this approach. Here, the D-A system could be understood as the dislocation core ascribed levels. The relative stability of the B-PL would be in good agreement with the dislocation core ascribed D-A transitions, where variation of dislocation density with epi-layer thickness can be assumed rather small for the identical growth regime.

C. Evaluation of the recombination and material parameters

Complicated redistribution of excess carriers among the radiative and non-radiative recombination centers in GaN layers has been revealed by the combining of the MW-PC and PL transient techniques. The observed two-componential MW-PC transients imply the non-exponential carrier decay process. A linearization of these residual MW-PC (after subtraction of the PL inherent component) transients is only possible using the stretched exponent approximation.[10,34,35] This approximation yields to a description of excess carrier density variations in time expressed as $n_{ex}(t) = n_{ex}(t=0)\exp[-(t/\tau_{se})^{\alpha}]$, where α is a fractional index which is associated with material disorder characteristics.[10,34,35] Fractional index is evaluated from a linear fit of the double logarithm of the normalized transients (Fig. 5) displayed on the logarithm time scale ($\ln(-\ln(U(t)/U(0)))$ versus $\ln(t)$).[34,35]

A rather good linearity of the normalized MW-PC signals approximated by a stretch-exponent is obtained (Fig. 5(a)) over a wide range of running time (form ns to ms) within a transient. The linearity is reached for the epi-layers of different thickness. However, the slopes of these lines in the plots are different. The slope increases with a thickness of epi-layer (Fig. 5(b)). This slope correlated with α can be associated with the fractal index.[25,34,35] The approach of α to unity implies a reduction of the disorder of material. Thereby, the crystalline structure slightly straightens up with enlargement of the thickness of GaN epi-layer over 15 μm. This result is in agreement with a reduction of the Y-PL intensity correlated with an increase of the epi-layer thickness (Fig. 4(d)).

Variation of the fractal index of an epi-layer (Fig. 5) is also correlated with the relative amplitude of an asymptotical component in the MW-PC transients (Fig. 6(a)) represented as a function of epi-layer thickness. The larger the relative amplitude of the asymptotic decay component is, the larger fraction of the excess carriers is involved into a random-walk/trapping within the inter-crystalline area, and the less fraction of the excess carrier density recombines in the micro-crystal volume. The relative amplitudes of the asymptotical component in the MW-PC transients obtained in the same thickness (2.5 μm) epi-layers (grown by using VU and TU MOCVD reactors) is compared in Fig. 6(a). It can be deduced that nearly the same quality of the GaN epi-layer is obtained if the growth regime is similar. However, the crystal quality is reduced under deviations from the optimal growth temperature regime. The stretch-exponent component within MW-PC transients correlates with manifestation of the traps responsible for the PL, - such a correlation can be deduced from comparison of the excitation intensity dependent changes of amplitudes of the asymptotic component in the MW-PC and PL transients, Fig. 3, and Y-PL transients, shown in Figs. 3(b) and 6(b).

For thin epi-layers, the impact of the surface recombination should always be evaluated. In the dislocation-rich thin samples, the surface recombination can be significant due to several reasons: i) the recombination on layer surfaces, ii) the recombination on dislocations cylinders (threading dislocations prevail), iii) the surface recombination on boundaries of a micro-crystal. The surface

Reuse of AIP Publishing content is subject to the terms at: https://publishing.aip.org/authors/rights-and-permissions. Download to IP: 158.129.154.116 On: Wed, 24 Aug 2016 07:35:45

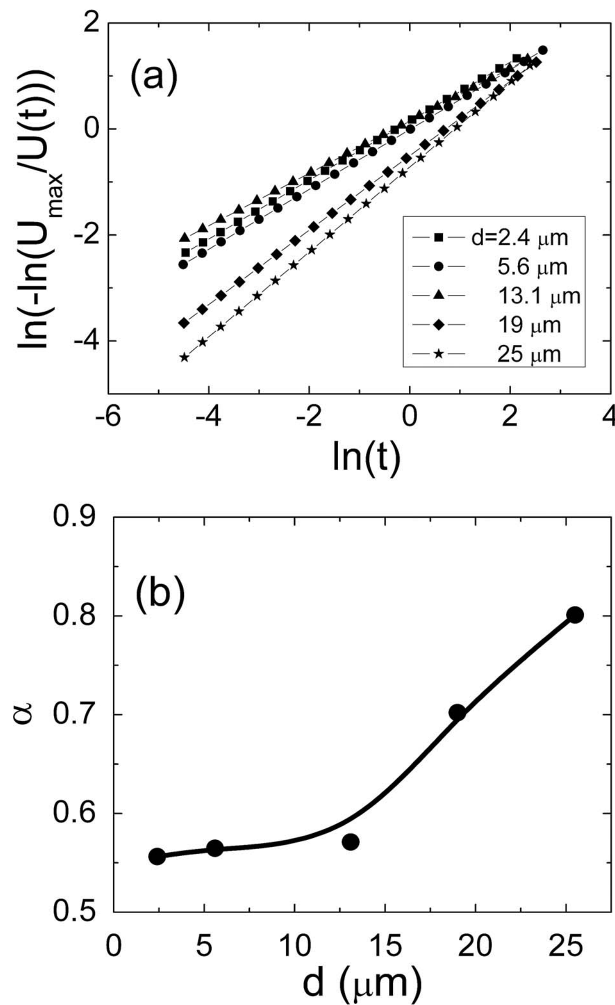

FIG. 5. Evaluation of the fractional index α by linearization of the normalized MW-PC transients at $I_{ex} \cong I_0$, ascribed to the non-radiative recombination (a), and variation of the fractional index as a function of epi-layer thickness (b).

recombination on the epi-layer interface/surface should be dependent on layer thickness d. Assuming the un-matched crystal cell constant at the interface between the GaN and sapphire, the largest surface recombination velocity s $\rightarrow \infty$ could be ascribed to this interface. For rather large surface recombination velocity, the recombination is limited by carrier diffusion to this interface. The shortest effective carrier decay lifetime τ_D is then evaluated as $\tau_D = d^{2/\pi^2} D \cong$ 1–125 ns for the entire range of layer thicknesses examined. Here, $D \geq 5$ cm^2/s is the coefficient of the carrier diffusion (estimated using the mobility values in Table I). The square symbols in Fig. 7 represent the simulated τ_D values calculated for the epi-layers examined as a function of layer thickness.

It can be noticed that the specific lifetime values cover the time scale from 1 ns to hundred of ns, measured at low excitation (pulsed) level $n/n_0 < 1$ (where excess carrier density n is significantly lower than equilibrium carrier density $n_0 > 3 \times 10^{16}$ cm^{-3}, Table I, i.e. $n \ll n_0$). However, the inherent lifetime values measured by MW-PC technique show the significantly longer characteristic times. Additionally, any clear dependence of the MW-PC decay on the epi-layer thickness was not revealed. The surface recombination on micro-crystal boundaries (which size can also be represented through $d = \phi$, with ϕ a diameter of a micro-crystal) can also be estimated by assuming very rapid surface recombination and using τ_D. The probable value of a diameter of the micro-crystals should be less than the thickness of a layer. Then, the simulated τ_D dependence on d is represented by a solid line in Fig. 7. It can be deduced from this dependence that the characteristic τ_D times should

Reuse of AIP Publishing content is subject to the terms at: https://publishing.aip.org/authors/rights-and-permissions. Download to IP: 158.129.154.116 On: Wed, 24 Aug 2016 07:35:45

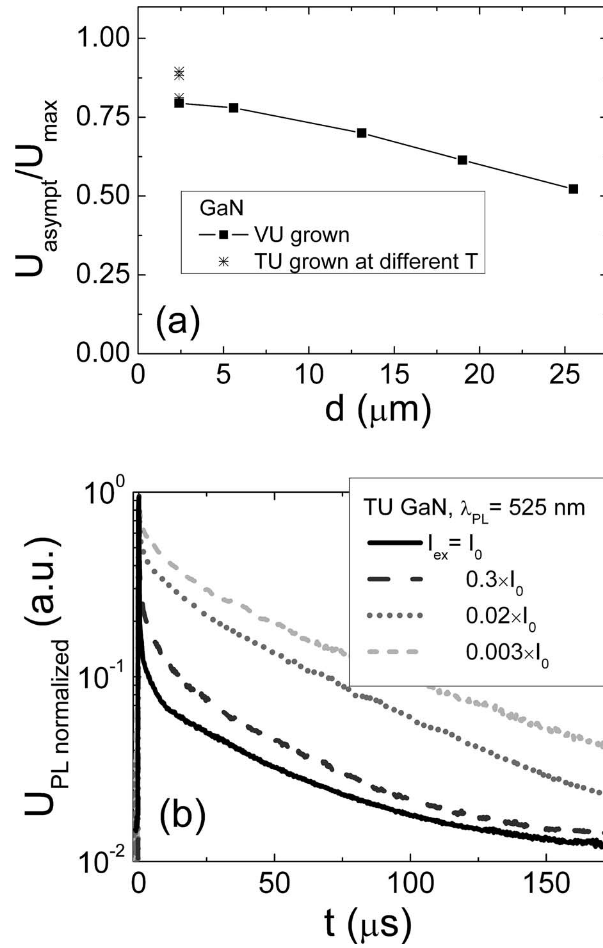

FIG. 6. (a)-Ratio of the amplitude of the asymptotic component in the MW-PC transient to peak amplitude of the residual MW-PC response as a function of an epi-layer thickness for $I_{ex} \cong I_0$. (b)-Variation of the Y-PL transients dependent on excitation density in the 2.4 μm –thick GaN 1047 sample.

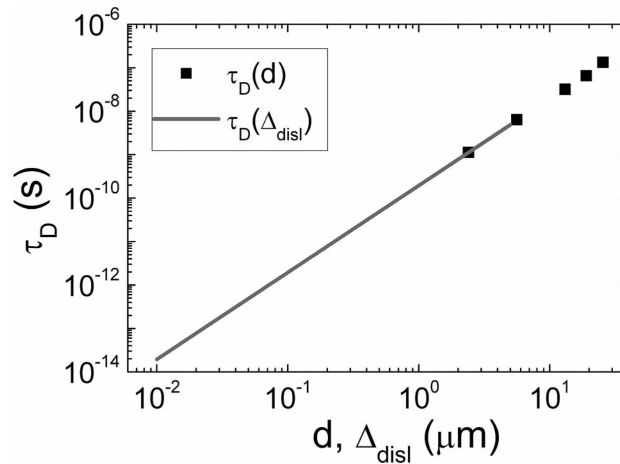

FIG. 7. Simulated lifetime (τ_D) of the diffusion limited surface recombination as a function of the epi-layer thickness (d) and of the effective distance ($\Delta_{dislocation}$) between the dislocations.

Reuse of AIP Publishing content is subject to the terms at: https://publishing.aip.org/authors/rights-and-permissions. Download to IP: 158.129.154.116 On: Wed, 24 Aug 2016 07:35:45

be shorter than 10 ns for the layers investigated. This is in good agreement with a range of the measured decay lifetimes for UV-PL and B-PL. Thereby, it can roughly be inferred that UV-PL is limited by the size of micro-crystals and the surface recombination on their boundaries, while B-PL is determined by the carrier (from the inter-crystalline area) recombination on the dislocations. For the recombination on the dislocations, the effective length $\Delta_{dislocation}$ can be estimated using a probable surface density N_{disl} of dislocations and assuming their nearly homogeneous (integrally) distribution, as $\Delta_{dislocstion} = N^{1/2}{}_{disl}$. A diameter of dislocation is determined by space charge region surrounding it. Really, this diameter can reach a measure of about 1 μm. Thereby, the largest density of dislocations is also limited, even for the compact deployment of micro-crystals and surrounding dislocations. The probable τ_D range due to $\Delta_{dislocstion}$ changes is again represented by a solid line in Fig. 7. Values of $\tau_D \sim$1–10 ns correlated with $N_{disl} \sim 10^8 - 10^{10}$ cm^{-2} (Table. I) agree with the experimentally observed range for the B-PL and the initial component of the MW-PC transients.

IV. SUMMARY

The microwave probed–photoconductivity (MW-PC) and spectrally resolved photoluminescence (PL) transients were simultaneously examined using an ultraviolet (UV) light 354 nm pulsed (500 ps) excitation. Analysis of the normalized MW-PC transients enabled us to distinguish the carrier decay components associated with carrier decay within micro-crystals and the disordered structure on the periphery areas surrounding crystalline columns. This examination combined with analysis of the PL spectral and temporal changes allowed for attribution of the trapping component, revealed in MW-PC transients, to the yellow Y-PL band in the range of $h\nu < 2.4$ eV. It has been obtained that intensity of UV- PL band increases with excitation density, while intensity of B-PL band is nearly invariant. The B-PL has been ascribed to carrier recombination on the dislocation cylinder surfaces. Fractional index α with values $0.5 < \alpha < 0.8$ was evaluated for the stretched-exponent component which fits the experimental transients determined by the disordered structure ascribed to the periphery areas surrounding the crystalline columns.

ACKNOWLEDGMENTS

This study was funded from the European Community's social foundation under Grant Agreement No. VP1-3.1-ŠMM-08-K-01-004/KS-120000-1756. T.M. acknowledges support of the Research Council of Lithuania under Post-doc program No. 004/14/MTDS-230000-395.

[1] S. Nakamura, T. Mukai, and M. Senoh, Appl. Phys. Lett. **64**, 1687 (1994).
[2] R. Schwarz, R. Cabeça, E. Morgado, M. Niehus, O. Ambacher, C. P. Marques, and E. Alves, Diamond & Related Materials **16**, 1437 (2007).
[3] M. Pophristic, F. H. Long, C. Tran, I. T. Ferguson, and R. F. Karlicek, J. Appl. Phys. **86**, 1114 (1999).
[4] S. Nagarajan, Y. S. Lee, M. Senthil Kumar, O. H. Cha, C.-H. Hong, and E.-K. Suh, J. Phys.D: Appl. Phys. **41**, 012001 (2008).
[5] P. J. Sellin and J. Vaitkus, Nucl. Instr. Meth. A **557**, 479 (2006).
[6] E. Gaubas, S. Juršėnas, R. Tomašiūnas, J. Vaitkus, A. Žukauskas, A. Blue, M. Rahman, and K. M. Smith, Nucl. Instr. Meth. Phys. Res. A **546**, 247 (2005).
[7] E. Gaubas, V. Kovalevskij, A. Kadys *et al.*, Nucl. Instrum. Meth. Phys. Res. B **307**, 370 (2013).
[8] E. Gaubas, K. Kazlauskas, R. Tomašiunas, J. Vaitkus, and A. Žukauskas, Appl. Phys. Lett. **84**, 5258 (2004).
[9] J. M. DeLucca, J. Appl. Phys. **88**, 2593 (2000).
[10] E. Gaubas, S. Juršenas, S. Miasojedovas, J. Vaitkus, and A. Žukauskas, J. Appl. Phys. **96**, 4326 (2004).
[11] V. V. Ursaki, I. M. Tiginyanu, P. C. Ricci, A. Anedda, S. Hubbard, and D. Pavlidis, J. Appl. Phys. **94**, 3875 (2003).
[12] E. Arslan, S. Butun, S. B. Lisesivdin, M. Kasap, S. Ozcelic, and E. Ozbay, J. Appl. Phys. **103**, 103701 (2004).
[13] D. Li, X. Dong, J. Huang, X. Liu, Zh. Xu, X. Wang, Z. Zhang, and Zh. Wang, J. Cryst. Growth **249**, 72 (2003).
[14] M. A. Reshchikov and H. Morkoç, J. Appl. Phys. **97**, 061301 (2005).
[15] M. Birkholz, *Thin film analysis by X-ray scattering* (Wiley-VCH Verlag GmbH&Co. KgaA, Weinheim, 2006).
[16] H. Heinke, V. Kirchner, S. Einfeldt, and D. Hommel, Appl. Phys. Lett. **77**, 2145 (2000).
[17] A. D. Kurtz, S. A. Kulin, and B. L. Averbach, Phys. Rev. **101**,1285 (1956).
[18] M. A. Moram and M. E. Vickers, Rep. Prog. Phys. **72**, 036502 (2009).
[19] N. M. Shmidt, V. V. Sirotkin, A. A. Sitnikova, O. A. Soltanovich, R. V. Zolotareva, and E. B. Yakimov, Phys. Stat. Sol. (c) **2**, 1797 (2005).
[20] E. B. Yakimov, J. Phys.: Condens. Matter **14**, 13069 (2002).
[21] K. Yamamoto, H. Ishikawa, T. Egawa, T. Jimbo, and M. Umeno, J. Cryst. Growth **189/190**, 575 (1998).

Reuse of AIP Publishing content is subject to the terms at: https://publishing.aip.org/authors/rights-and-permissions. Download to IP: 158.129.154.116 On: Wed, 24 Aug 2016 07:35:45

[22] R. A. Smith, *Semiconductors* 2nd ed. (Cambridge University Press, Cambridge, 1978).
[23] K. L. Luke and L. J. Cheng, J. Appl. Phys. **61**, 2282 (1987).
[24] E. Gaubas, J. Vaitkus, E. Simoen, C. Claeys, and J. Vanhellemont, Mater. Sci. Semicond. Process. **4**, 125 (2001).
[25] S. Havlin and D. Ben-Avraham, Advances in Physics **51**, 187 (2002).
[26] M. Gallart, T. Taliercio, A. Alemu, P. Lefebvre, B. Gil, J. AlleÁgre, H. Mathieu, and S. Nakamura, Phys. Stat. Sol. (b) **216**, 365 (1999).
[27] S. F. Chichibu, H. Marchand, M. S. Minsky, S. Keller, P. T. Fini, J. P. Ibbetson, S. B. Fleischer, J. S. Speck, J. E. Bowers, E. Hu, U. K. Mishra, and S. P. DenBaars, Appl. Phys. Lett. **74**, 1460 (1999).
[28] G. Pozina, N. V. Edwards, J. P. Bergman, B. Monemar, M. D. Bremser, and R. F. Davis, Phys. Stat. Sol. (a) **183**, 151 (2001).
[29] J. Mickevičius, M. S. Shur, R. S. Fareed, J. P. Zhang, R. Gaska, and G. Tamulaitis, Appl. Phys. Lett. **87**, 241918 (2005).
[30] S. Juršėnas, S. Miasojedovas, G. Kurilčik, A. Žukauskas, and P. R. Hageman, Phys. Stat. Sol. (a) **201**, 199 (2004).
[31] B. Monemar, P. P. Paskov, J. P. Bergman, G. Pozina, A. A. Toropov, T. V. Shubina, and T. Malinauskas, Phys. Rev. B **82**, 235202 (2010).
[32] P. P. Paskova, R. Schifano, T. Paskova, T. Malinauskas, J. P. Bergman, B. Monemar, S. Figge, and D. Hommel, Physica B **376–377**, 473 (2006).
[33] B. Monemar, P. P. Paskov, J. P. Bergman, T. Paskova, C. Hemmingsson, T. Malinauskas, K. Jarasiunas, P. Gibart, and B. Beaumont, Physica B **376–377**, 482 (2006).
[34] J. C. Phillips, Journal of Non-Crystalline Solids **357**, 3853 (2011).
[35] J. C. Phillips, Rep. Prog. Phys. **59**, 1133 (1996).

Reuse of AIP Publishing content is subject to the terms at: https://publishing.aip.org/authors/rights-and-permissions. Download to IP: 158.129.154.116 On: Wed, 24 Aug 2016 07:35:45